Damage detection in beams from modal and wavelet analysis using a stationary roving mass and noise estimation

M. Solís, Q. Ma and P. Galvín

Escuela Técnica Superior de Ingeniería, Universidad de Sevilla, Camino de los Descubrimientos, Sevilla 41092, Spain

ABSTRACT: This paper uses the Continuous Wavelet Transform Analysis on mode shapes for damage identification. The wavelet analysis is applied to the difference in the mode shapes between a healthy and a damaged state. The paper also includes a novel methodology for estimating the level of noise of the experimental mode shapes based on a standard Signal to Noise Ratio (SNR). The estimated SNRs are used for identifying and making emphasis on the less noisy data. Moreover, a mass attached to the structure is considered to enhance the sensitivity of the structure to damage. Modal analysis is performed for different positions of the mass along the beam. The results obtained for all the positions of the mass are combined so an averaging process is implicitly applied. The paper presents the results from an experimental test of a cantilever steel beam with different severity levels of damage at the same location. The results show that the use of the attached mass reduces the effect of noise and increases the sensitivity to damage. Little damage can be identified with the proposed methodology even using a small number of sensors and only the first five bending modes.

KEY WORDS: Damage detection and localization, beams, wavelet analysis, modal analysis, structural health monitoring

Introduction

It is well known that the presence of damage (cracks) in a beam implies a change in its dynamic properties. Based on this fact, vibration based damage detection techniques try to detect the presence of damage by analyzing the change in natural frequencies, mode shapes and/or damping ratios. Some pioneering damage detection techniques [1] were based on the analysis of changes in natural frequencies, which are the most simple dynamic parameters to be measured. However, the natural frequencies are not sensitive to damage. Only a significant damage would induce a significant change in the natural frequencies. Moreover, the effect of damage may be masked by the effect of changes on environmental conditions, experimental noise, uncertainties, etc. On the other hand,

natural frequencies are a global parameter of the structure, and therefore they can only provide information about the presence of damage but not about its location. In order to locate damage, the mode shapes of the structure may be used. From an experimental point of view, the identification of mode shapes requires a larger amount of sensors (more complex and expensive experimental set-ups) as well as more sophisticated system identification methods. This paper uses traditional piezoelectric accelerometers for the experimental modal analysis. However, it should be noted that developing Fiber Bragg Grating (FBG) sensors provide advantages for practical applications because of their light weight and multiplexing capabilities. Thus, the use of FBG sensors is rapidly increasing in the last years within the Structural Health Monitoring (SHM) community (see for instance [2, 3]). Despite of the experimental and mathematical efforts for modal identification, the changes in mode shapes induced by damage are usually subtle (unless severe damage is present) so damage can not be identified from mode shapes in a straightforward way. There is a significant number of papers that propose different techniques and damage detection parameters to analyze the information provided by mode shapes [1].

The wavelet transform is a rather new mathematical tool that has been developed from the 90s for signal processing and information encoding [4]. The wavelet transform is sensitive to local changes in the original signal. The wavelet coefficients show a singular behavior, ridges or peaks, when a discontinuity or a sudden change occurs. Thus, they can be used as an indicator of damage when applied to mode shapes, assuming that damage leads a discontinuity in mode shapes. Several authors have made different proposals to damage detection in structures by applying wavelet transform to mode shapes, time response, static deflection, etc., after the pioneering work by Surace and Ruotolo [5]. The state-of-the-art in wavelet transform exploring the possibilities of this technique for SHM was reviewed by Taha et al. [6] and Katunin [7]. The researches have been focused on the choice of the wavelet function, the severity of the identified defect, the experimental noise and the spatial sampling interval (i.e. the number of sensors).

For beam type structures, Rucka [8] presented a numerical and experimental study of a cantilever beam with damage depth of 20%, 10% and 5% of the beam height. She analyzed the first eight mode shapes and the influence of the mode order on the effectiveness of damage detection by the Continuous Wavelet Transform (CWT). From this analysis, the smallest detectable defect was found to be of a depth of 10% of the beam height and its localization was only possible at higher vibration modes. Moreover, the methodology was more effective using wavelets with smaller numbers of vanishing moments. Cao et al. [9] used the wavelet transform coupled with the Teager energy operator to detect multiple damage in beams. The methodology is based on the curvature mode shapes since this parameter showed stronger immunity to noise and greater sensitivity to damage. The authors identified multiple damage of small dimensions in beams in high-noise conditions from this approach. Recently, Ulriksen and Damkilde [10] introduced a damage localization method composed of two signal processing steps, a CWT and the application of a generalized discrete Teager Kaiser energy operator, and a subsequent statistical evaluation step to discriminate between damage-induced discontinuities and other signal irregularities. The authors showed the applicability of the method in the context of an experimental work with a scaled wind turbine blade. This

methodology requires a relatively fine measurement density.

For two dimensional structures, Rajendran and Srinivasan [11] studied the detection of damage, modeled as an added mass, in glass fiber reinforced polymer plates employing two-dimensional wavelet packet transform, using rotational mode shape as an input. The proposed algorithm was sensitive to damage in a noisy environment with 5% noise. Katunin and Przystaka [12] presented an approach for damage identification in composite plates based on the fractional wavelet transform of modal displacements. They improved the sensitivity of the method by considering spatial fractional B-spline wavelets with optimized parameters. After, Katunin et al. [13] presented a method for automated damage identification and classification from the computed tomography scans using a wavelet-based algorithm. The authors tested two plates made of composite materials. The plates contained damages produced by cutting the circular holes by the water-jet method. The advantage of this methodology is the possibility of automated extraction and classification of predefined types of defects and it is also possible to evaluate the direction of damage propagation. Later, Katunin [14] proposed a method for the identification of damages in cross-ply epoxy laminated plates reinforced with E-glass cloth caused by stone impacts using wavelet analysis of modal data with quincunx non-separable wavelets. The obtained results showed that the impact damages, both cracks and delaminations, are well recognizable for even low energies of an impact. The main advantage of the application of quincunx wavelets of optimally selected fractional order for damage identification was the increasing sensitivity of the method with simultaneous decreasing of the computational time.

Regarding the required number of sensors, Montanari et al. [15] examined the effect of the spatial sampling interval in damage detection by CWT. A parametric study was carried out by analyzing the first three mode shapes of two set-ups for a beam varying the sampling interval, the noise level, the padding method, the wavelet function, the crack depth and position along the beam, and the mechanical and geometrical beam parameters. The coiflet wavelet function with four vanishing moments was found to be the most effective one. The authors determined the minimum optimal number of sampling points in relation to the beam deflection shape and the damage location.

Solis et al. [16] have previously proposed a simple damage detection technique based on the wavelet analysis of the difference in mode shapes between a healthy and a damaged state. The main idea of this technique is to combine all the information provided from the wavelet analysis of all the identified mode shapes and the natural frequencies by a weighted addition of the wavelet coefficients according to the changes in the natural frequencies for each mode. This methodology was successfully applied to cracked steel beams. In this paper, the authors include some new ideas for making the proposed damage detection method more robust and sensitive to little damage.

Firstly, a mass is attached to the structure and modal analysis is performed for different positions of the mass. The mass is at a fixed position for each experimental test (it is not a moving load) but it changes its position from one test to another. Zhong and Oyadiji [17, 18] previously used this idea for damage detection in beams and first used the term 'stationary roving mass'. This term is also used in this paper as an acknowledgement. The response of the damaged beam depends on its stiffness, mass distribution and boundary conditions. Hence, the presence of the additional mass changes the modal properties (natural frequencies and mode shapes) of the beam. The

natural frequencies and mode shapes from all the mass positions are analyzed in order to enhance the sensitivity to damage: at some positions of the mass, the dynamic response of the beam (and therefore its modal properties) is more affected by the presence of the mass so it is easier to detect the damage if compared to the situation in which no mass is added. Secondly, an estimation of the level of noise for each mode (Signal to Noise Ratio (SNR)) is performed by comparing the experimental mode shapes with a set of reference mode shapes obtained from a smoothed spline interpolation of the experimental mode shapes. The mode shapes that exhibit a higher SNR are considered more reliable for damage detection and their information should be specially analyzed. Finally, the proposed methodology combines the information obtained from all positions of the roving mass and the estimated SNRs. It analyzes the results for each mode individually and also for all the modes together.

The outline of the paper is as follows. Firstly, the proposed damage detection method is described from a mathematical and practical point of view. Secondly, the experimental work is described and the experimental results are presented and discussed. Finally, some conclusions are drawn.

Mathematical definition of the proposed damage detection method

The proposed damage detection method is based on the wavelet analysis of mode shapes. The CWT of a function $f(x)$ can be defined as:

$$CWT_f(u,s) = \frac{1}{\sqrt{s}} \int_{-\infty}^{+\infty} f(x)\Psi^* \left(\frac{x-u}{s} \right) dx \tag{1}$$

where Ψ is the wavelet function. Expression (1) is a convolution integral in which the resulting wavelet transform depends on two fundamental parameters of the wavelet function: the translation parameter (u) and the scale parameter (s). By changing the translation parameter, the wavelet function 'moves' along the x coordinate, whereas by changing the scale parameter, the wavelet function stretches or shrinks. In the end, the values of the resulting wavelet transform indicate how similar is the original function to the wavelet function for each value of the translation and scale parameters. A more in depth description of the mathematics of the wavelet transform and its applications can be found elsewhere [6, 10, 16, 19, 20, 21].

From a structural damage detection perspective, the usefulness of the wavelet analysis is that it is sensitive to local and subtle changes in the original signal. Thus, it can be used for instance to indicate the effect of damage on mode shapes, since the changes induced by damage will induce a singular behavior of the wavelet coefficients (local increase on their values). The selection of the wavelet function can affect the obtained results. The shape of the wavelet function should be as close as possible to the change induced by damage, so the wavelet coefficients exhibit the highest values at damage locations. However, it is not usually feasible to know the actual effect of damage. In most applications, the choice of the wavelet function is made by trial and error or based on previous applications (a review of different used wavelets can be found in previous works [6, 22]). There are also some papers that have addressed this issue from a more rigorous mathematical point of view [7, 8, 12, 19], but up to now there is a lack of a

robust criteria for selecting the best wavelet function. In a previous work [16], where an open crack was also introduced on a steel beam, the authors compared the results obtained with Daubechies, Gauss and Symlet wavelets with 2 and 3 vanishing moments. Daubechies wavelet was more sensitive to damage and provided better results, so Daubechies wavelet with 2 vanishing moments is chosen in the present analysis, as the type of damage is similar to the previous work.

The wavelet coefficients of the wavelet function are related to the derivatives of the input signal of the same order as the number of vanishing moments of the wavelet function [23, 24, 25]. Therefore, by selecting 2 vanishing moments, the CWT coefficients of mode shapes differences give information about the change in the second derivatives of mode shapes (modal curvatures) which is a well-known sensitive feature for damage detection. Thus, the relation between the obtained wavelet coefficients using a Daubechies wavelet with 2 vanishing moments and the changes in modal curvatures justifies the sensitivity of the proposed methodology to damage. However, this paper also shows results obtained with other wavelets in order to validate the wavelet choice.

The proposed methodology applies the wavelet transform to detect changes in the dynamic properties of the structure between two different states: a reference state and a possible damaged one. Thus, the wavelet transform is applied to the difference between the damaged mode shape and the undamaged one (Φ^i_{diff}) for each mode i:

$$CWT^i_{\Phi_{diff}}(u,s) = \frac{1}{\sqrt{s}} \int_{-\infty}^{+\infty} \Phi^i_{diff}(x) \Psi^* \left(\frac{x-u}{s} \right) dx \tag{2}$$

In order to avoid the so-called edge effect in the wavelet transform, an anti-symmetric extension of the signal is applied at both of its ends [4, 16]. When analyzing the wavelet coefficients, only those corresponding to the original part of the mode shapes are considered, whereas those out of that part (that are affected by the edge effect) are disregarded. On the other hand, the mode shapes are also mathematically transformed through a cubic spline interpolation. This transformation reduces the influence of the experimental random and local noise, which is a major concern when trying to identify the effect of a potential damage that may be masked by noise. It also allows to obtain additional modal information at interpolation points, which allows obtaining a more clear information from wavelet analysis [10, 16, 21, 26].

The wavelet coefficients obtained from Expression (2) are usually plotted in a 2D colored picture (scalogram) where the axes are the positions along the beam and the scale. The colors in the picture indicate the values of the coefficients for each position and scale. This paper applies a simple tool proposed by the authors to analyze the coefficients for all scales in one single picture [16]. It consists of the use of absolute values and the normalization to the maximum value for each scale. If no normalization is performed, higher values are obtained for higher scales, so no information about the singularities and ridges can be observed from the color map of the scalogram for low scales. By normalizing the values for each scale, one can see the oscillations appearing at each scale and the effect of damage can be more easily detected. Therefore, when the coefficients from all modes are combined and normalized for each scale, the effect of damage can be noticed for all scales and is clearly detected when maximum values (unity) are obtained for every scale at a certain location. The actual mathematical

meaning of the wavelet coefficients is lost with the normalization process, but this is irrelevant since they are used as a relative indicator of the presence of damage, and no interpretation is obtained from their actual numerical values.

This paper also introduces the attachment of a mass to the structure at certain positions along the beam, so the mode shapes are obtained for all those positions. It should be noted at this point that the structure changes (the mass distribution changes) when the mass is moved from one position to another. However, an experimental modal analysis is performed for each position of the mass for the reference and for the damaged state and the wavelet transform is applied to the difference in mode shapes for each mass position. Therefore, the difference in the mode shapes is theoretically (if there is no noise effect) coming only from the effect of damage and not from a different mass distribution. The change induced by the mass position is consequently canceled out, and all the performed wavelet analysis are consistent and pointing to the damage location, and not to the mass position. At each step of the wavelet analysis, the analyzed structure is the same, except for the damage. In addition, the added mass will emphasize the effect of damage at certain positions. However, it is not feasible from a practical point of view to predict which are the most relevant positions of the mass for damage detection. Actually, they will depend on the damage position, the mode shape and the boundary conditions. Thus, the results obtained for each position are combined in a single scalogram by adding up the scalograms for each mass position. This addition reduces the effect of the random noise in the mode shapes along the beam. It also allows considering more favorable scenarios for damage detection when compared to the situation where no roving mass is considered, because of the amplification of the effect of damage for some positions of the mass. Moreover, the attached mass can also provide some additional benefits in real applications. For instance, it can enforce cracks to be permanently opened during the tests, so its effect can be more easily identified.This can be specially advantageous for prestressed beams, in which the effect of a crack on the dynamic properties of the beam is reduced [27, 28]. However, the effect of the roving mass should be specifically analyzed since the sensitivity of the methodology could be affected depending on the capability of the mass to keep the crack open or not during the tests.

When computing the addition of wavelet coefficients, the authors proposed in a previous work [29] that the coefficients are weighted through a coefficient based on the shift in natural frequency between the reference and the damaged state. Since the change in natural frequency is an indicator of how the damage has affected the structure, then the information coming from the most affected mode shapes is emphasized.

In addition to that, this paper also introduces a novel weighting parameter for the addition of wavelet coefficients. It is based on the estimated noise of each mode, so the less noisy mode shapes are also emphasized. The noise in mode shapes is a key issue affecting the sensitivity to damage. If no noise is present, the proposed method is extremely sensitive to little damage [29]. Therefore, the sensitivity to damage is enhanced by estimating the noise level on the mode shapes in order to evaluate their accuracy and subsequently highlight the information provided by the less noisy mode

shapes. Thus, for a single mode i, the resulting scalogram can be computed as:

$$CWT^{i}_{sum}(u,s) = \sum_{j=1}^{M} \left| CWT_{\Phi^{ij}_{diff}}(u,s) \right| \cdot \left(1 - \frac{\omega^{ij}_{u}}{\omega^{ij}_{d}} \right)^{2} \cdot \text{SNR}_{ij} \tag{3}$$

where subindex j is related to each position of the added mass, ω_u and ω_d are the natural frequencies for the undamaged and damaged states respectively, and SNR_{ij} is the estimated Signal to Noise Ratio. The obtained normalized scalogram ($CWT^{i}_{sum\_norm}$) is obtained from Equation (4) and it can be used for analyzing the information provided by mode i for damage detection.

$$CWT^{i}_{sum\_norm}(u,s) = \frac{CWT^{i}_{sum}(u,s)}{max|CWT^{i}_{sum}(u,s)|_{s}} \tag{4}$$

The SNR_{ij} is defined in its usual form for experimental data analysis [30]:

$$\text{SNR}_{ij}[\text{dB}] = 10 \log \left(\frac{P^{ij}_{mode}}{P^{ij}_{noise}} \right) \tag{5}$$

where P^{ij}_{mode} is the power of the mode shape i for the mass position j, defined as the square of its Root Mean Square value:

$$P^{ij}_{mode} = \frac{\sum_{k=1}^{n} {x^{ij}_{k}}^{2}}{n} \tag{6}$$

where x^{ij}_{k} is the kth component of the mode shape vector and n is the number of its components, and P^{ij}_{noise} is the estimated power of the noise:

$$P^{ij}_{noise} = \frac{\sum_{k=1}^{n} \left(x^{ij}_{k} - {x^{ij}_{k}}^{ref} \right)^{2}}{n} \tag{7}$$

where ${x^{ij}_{k}}^{ref}$ is the kth component of a reference noise-free mode shape vector. In this paper, the cubic spline interpolation of the corresponding mode shape i for the mass location j is used as a reference noise-free mode.

The previous definition of the SNR is usually applied to experimentally acquired signals. In this case, the mode shapes are considered as noisy experimental signals, although they are not a directly acquired experimental signal. The noise in mode shapes comes from the original noise of the accelerometers and impact hammer signals, and also from the numerical process of the modal analysis. At this point, it should be noted that wavelet analysis is well-known mathematical tool for denoising signals (usually the Discrete Wavelet Transform). Therefore, it could be also used for filtering the acquired recordings from the sensors and increase their resulting SNR [31, 32]. However, this enhancement is not likely to have a significant effect on the identified mode shapes since no filtering should be applied at frequencies close to the natural frequencies of the structure. On the other hand, this paper is interested in the SNR of the mode shapes and

not of the signals from the accelerometers. Then, the Continuous Wavelet Transform is applied for detecting changes in mode shapes induced by damage and not for denoising.

The normalized scalogram obtained for each experimentally identified mode shape can be analyzed separately in order to look for potential damage effects. Unfortunately, not all the modes may be sensitive to damage. Some of them may clearly indicate the presence of damage whereas some others do not exhibit any influence from damage and they may show irregular behavior of the wavelet coefficients because of the noise. In real applications, where the actual position of the damage is not really known, it may not be possible to distinguish between the effect of noise and the effect of damage and eventually to properly choose the mode shapes that are really sensitive to damage. The results from the less noisy mode shapes is more accurate, and especially in those regions where they exhibit maximum modal amplitudes, since those regions are more sensitive to damage.

Finally, the information coming from all the identified mode shapes can also be combined to obtain a global result that can also provide some additional information about the presence of damage and also some implicit information on which mode is more reliable and sensitive to damage, as far as it is similar to the result obtained with any individual mode:

$$CWT_{sum}(u,s) = \sum_{i=1}^{N} CWT^{i}_{sum}(u,s) = \sum_{i=1}^{N}\sum_{j=1}^{M} \left| CWT_{\Phi^{ij}_{diff}}(u,s) \right| \cdot \left(1 - \frac{\omega^{ij}_{u}}{\omega^{ij}_{d}} \right)^{2} \cdot \mathrm{SNR}_{ij} \tag{8}$$

where subindex i and j are related to each mode shape (N is the number of experimentally identified mode shapes) and each position of the added mass (M is the number of positions considered for the mass), respectively, whereas u and d stand for the undamaged and the damaged case, respectively. The final scalogram obtained from Equation (8) is also normalized for every scale according to Equation (9), and the obtained normalized scalogram ($CWT_{sum\_norm}(u,s)$) can be used to analyze the whole information from all the identified mode shapes in just one single picture.

$$CWT_{sum\_norm}(u,s) = \frac{CWT_{sum}(u,s)}{max|CWT_{sum}(u,s)|_{s}} \tag{9}$$

It is worth to mention at this point that the normalization process of Equations (4) and (9) are carried out after the addition is performed for all positions of the mass, and after the addition for all positions of the mass and all the mode shapes, respectively. Therefore, during the addition process, the original values of the wavelet coefficients are kept, so the relative differences between different mode shapes and mass positions are kept, though they are modulated through the weighted coefficients related to the shift in natural frequencies and SNR.

The interpretation of the normalized scalogram for damage detection is further discussed from a practical point of view in the following section, where experimental damage detection results are presented.

Experimental results

Test set-up and experimental modal analysis

This section presents the experimental results obtained for a steel cantilever beam with a cross section of 30 mm $\times$ 10 mm and a length (L) of 800 mm. Figure 1 shows pictures of the real test and a scheme of the tested beam. The damage is artificially induced by a saw cut (2 mm width approximately through all the beam width) at a distance of $0.4L$ from the fixed end of the beam. Increasing depths of the cut were considered during the experimental campaign: 1 mm, 2 mm and 5 mm depths that correspond to 10%, 20% and 50% of the height of the beam are the three damage scenarios.

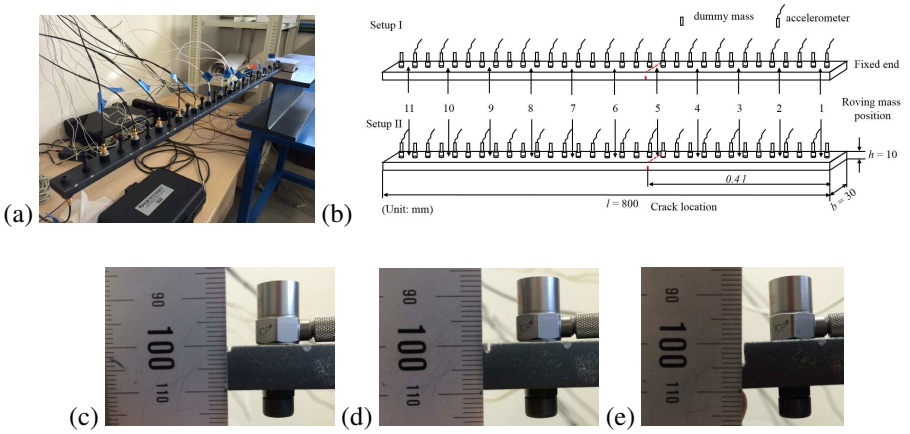

Figure 1: (a) Picture of the experimental setup (b) scheme of the tested beam (c) 10% crack (d) 20% crack (e) 50% crack.

The dynamic response of the beam was measured at 32 measuring points by using two set-ups of 16 roving accelerometers (general purpose piezoelectric type with 100mV/g nominal sensitivity and a mass of 4 grams). The measuring points were distributed along the beam every 25mm leaving 10mm from the fixed and from the free end. The accelerometers were located at the odd positions in one set-up and at the even positions in the other. The accelerometers were fixed to the beam through a threaded screw.

The location of the damage is just in the middle of two adjacent measuring points, which is a demanding situation for damage detection. If the damage location was coincident with a measuring point, the damage would be more easily identified [16].

Two different values of the attached mass have used for the tests: a 5% and a 10% of the total mass of the beam (1.884kg). In this case, an aluminium device was designed to be hanged from the beam at different positions, as shown in Figure 2. Eleven equally distributed positions were considered along the beam.

The excitation force is applied at the free end of the beam with an impact hammer and the averaged Frequency Response Functions (FRFs) are obtained from 5 impacts for the 16 measuring points of each set-up. The mode shapes and natural frequencies are

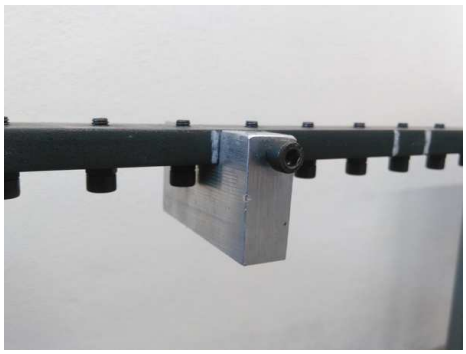

Figure 2: Picture of the added roving mass.

identified by applying the Poly-reference Least Squares Complex Frequency Domain (plSCF) algorithm [33] to the FRF matrix of the whole beam (32 measuring points) obtained from the assemble of the FRF matrices of both set-ups. Table 1 shows the identified first five natural frequencies for each damage scenario and the reference state and Table 2 shows the Modal Assurance Criterion (MAC) values of each mode shape between its damaged and reference states. Figure 3 illustrates the obtained FRFs by showing the results at the free end of the beam for the undamaged and the damaged states. For the sake of brevity, these tables and figure include only the results without roving mass. Similar values and conclusions are obtained with the roving mass attached at all different positions. From the tables, it can be seen that the change of natural frequencies induced by damage, even for a 50% crack, is less than 2%, so the damage can not be detected from such a global and simple parameter. The MAC values are all higher than 0.98, which means that they are very well correlated and similar to each other. Figure 3 also shows that the effect of damage is very little on the structural response. The FRF for each damaged state is very similar to the undamaged situation. Only a slight shift in the natural frequencies is observed for the 50% crack.

Figure 4 shows the five identified mode shapes for the undamaged and the 50% damage scenarios without the roving mass. Modes shapes are normalized to unit maximum amplitude in order to obtain a more consistent information from different states of the beam (different damages and mass positions). It can be seen that the effect of damage is negligible in the mode shapes even for such a severe damage, so any advanced mathematical analysis (for instance wavelet analysis) is necessary to detect the subtle and local changes induced by damage. From a practical point of view, it should be mentioned at this point that because of the light weight of the structure, even the small mass of the attached accelerometers (4 grams) influence the dynamic response of the structure. This effect would not be relevant if all the accelerometers were always at a fixed position, because their effect would be the same in both the reference and the damaged state. For the same reason, the holes and their corresponding screws for attaching the accelerometers do not affect the damage detection results, since they are always present. However, because of the slightly different distribution of the mass of

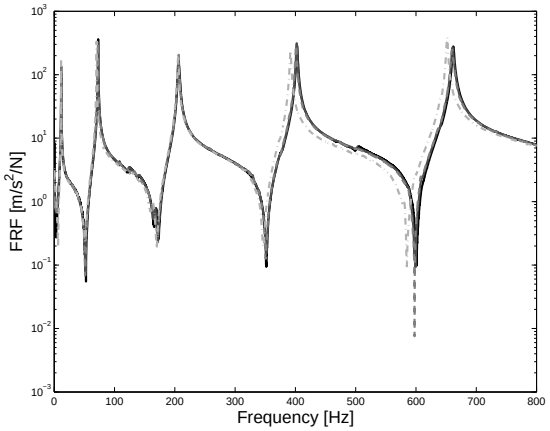

Figure 3: FRF of the free end of the beam for the undamaged (solid black line), 10% crack (solid gray line), 20% crack (dashed gray line) and 50% crack (dashed-dotted gray line) states (no added mass).

the accelerometers for each set-up, the identified mode shapes for the two set-ups did not match properly between each other. In order to solve this issue, equivalent dummy masses were added at each measuring point where no accelerometer was present at each set-up. These additional masses consisted of an additional nut and a screw attached to the screw at each measuring point where an accelerometer was not present for each set-up (Figure 5). It can be seen in Figure 4, therefore, that no discontinuity can be observed in the mode shapes because of a different mass distribution for the two set-ups. On the other hand, the cables (Figure 1(a)) were hanged from an auxiliary structure to minimize their effect on the beam response.

Table 1: Experimental natural frequencies [Hz] for each damage scenario (no added mass).

Mode\Scenario	Intact	10%	20%	50%
1	11.70	11.68	11.64	11.53
2	72.97	72.68	72.53	70.43
3	206.63	206.44	206.41	205.47
4	402.84	402.28	401.02	391.87
5	662.47	661.21	660.04	651.52

Figure 4 shows that the experimental noise is apparently very small for modes 2 to 5. The mode shapes are smooth and well identified. However, both the undamaged and 50% damage states show appreciable noise in mode 1. An hypothesis for the noise in mode 1 is an imprecise operation of the accelerometers in such a low frequency range. Nevertheless, this noisy information will serve as a proof of the ability of the proposed methodology to detect damage even when some noisy results are obtained, as it will be discussed in the next section.

Table 2: MAC values of each mode of each damage scenario with the corresponding undamaged one (no added mass) damage scenario.

Mode\Scenario	10%	20%	50%
1	0.9879	0.9966	0.9981
2	0.9999	0.9997	0.9994
3	0.9997	0.9995	0.9993
4	0.9996	0.9995	0.9975
5	0.9997	0.9978	0.9931

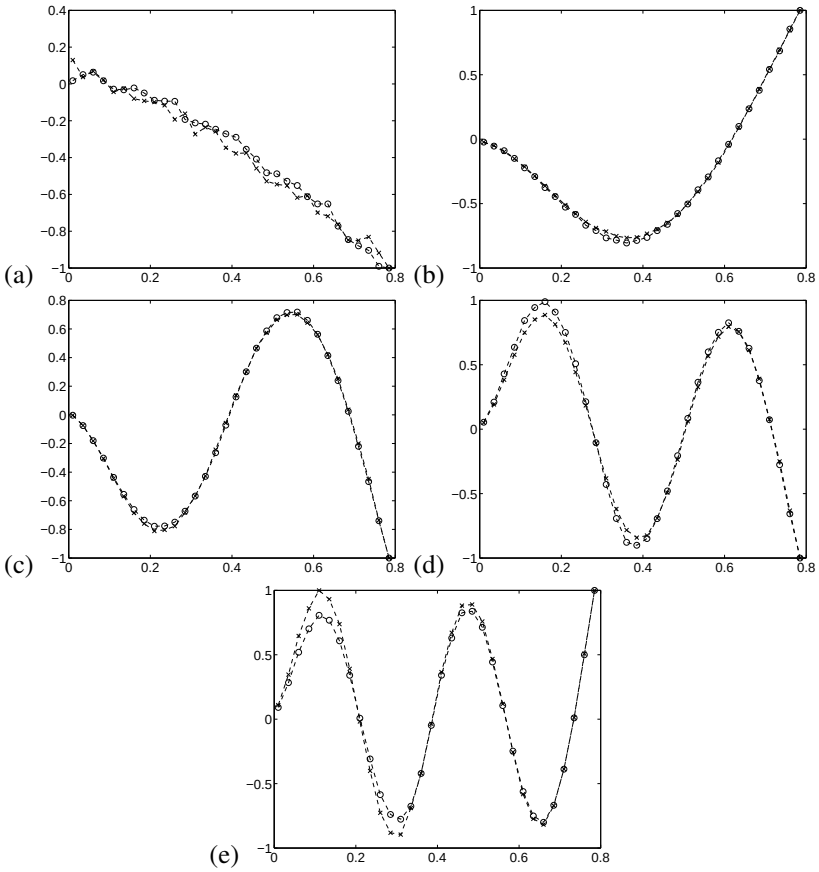

Figure 4: Identified mode shapes for the undamaged (-x-) and the 50% damage (-○-) state (no roving mass)

At this point, the actual level of noise in the experimental results is estimated by comparing the experimentally identified mode shapes with numerically obtained mode shapes for the undamaged state. This preliminary analysis is useful to identify which

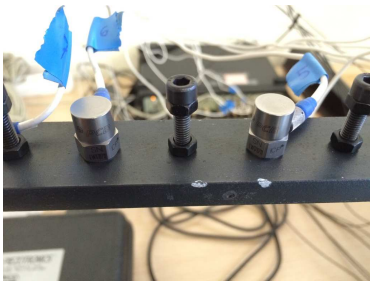

Figure 5: Picture of the accelerometer and the dummy accelerometer masses

modes are expected to be more reliable for damage detection. In addition, the estimation of this real level of noise can be useful for comparison purposes with future researches and also for providing reference values in researches where artificial noise is introduced to numerically obtained mode shapes. Firstly, a numerical model is developed including the non structural masses (roving mass, mass of the accelerometers and dummy masses) as well as a rotational spring at the fixed end of the beam, in order to match as closely as possible the experimental results. The model is built using a Matlab toolbox developed by Yang [34]. An optimum value of $1.8 \cdot 10^5$ Nm/rad was found for the stiffness of the rotational spring by a manual calibration. Table 3 shows the MAC values between the experimental and the analytical mode shapes for all positions of the roving mass. Figure 6 illustrates how similar are the experimental and numerical mode shapes by showing them when no roving mass is present. The very high values of MAC and the mode shapes from Figure 6 show that the numerical model represents very accurately the real test. Thus, the numerical modes can be considered as a set of reference noise free modes to estimate the SNR of the experimental mode shapes by applying Equations (5), (6) and (7).

The obtained SNR values are shown in Table 4. The estimated values are in the range $40 - 70$ dB. It can be seen mode 2 is clearly the least noisy (highest SNR values) and it is expected to be the most reliable mode for damage detection. In practical applications, building a reliable model of the undamaged structure might not be feasible. In addition, modeling the damaged state is even more difficult since the location, and severity of damage is unknown, unless a model updating process is carried out. Since the proposed methodology is aimed at being model-free and avoid complex modeling strategies, it is proposed to use the cubic spline approach of each experimental mode shape as the reference noise-free mode shape. In order to evaluate the performance of the proposed strategy, the SNR values obtained from the proposed method for the undamaged beam are shown in Table 5. It can be seen that the values of Tables 4 and 5 are similar. Thus the proposed methodology is valid for estimating the SNR of the mode shapes.

Damage detection

In this section, the results obtained for each damage scenario are presented. The resulting scalograms for each mode and for the combination of all modes are analyzed. Each

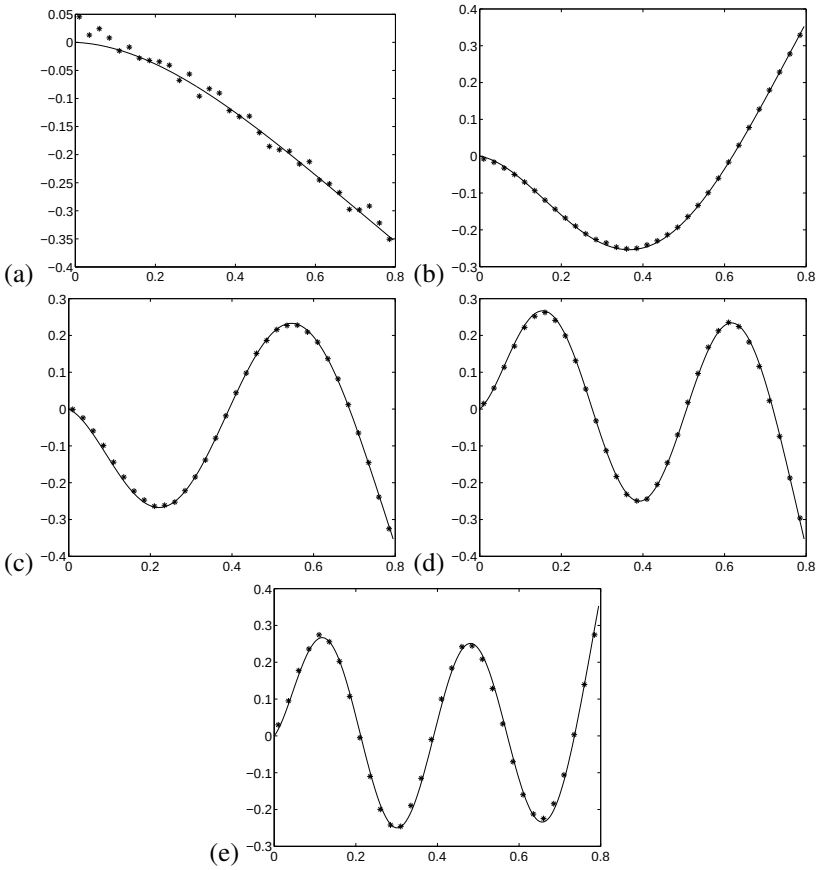

Figure 6: Experimental ($*$) and numerical (solid line) mode shapes of undamaged state (no roving mass).

result is defined by the depth of the crack (expressed in % of the beam height) and the value of the roving mass (expressed in % of the mass of the beam).

For the damage identification from the scalograms, it must be pointed out that the effect of damage is present at every scale, whereas the effect of noise (experimental noise in the sensors, uncertainties in the modal identification process, numerical instabilities in the interpolation process, etc.) affects only certain scales. This phenomenon has been reported and addressed in previous works [35, 36]. Therefore, a singular behavior (peak or ridge) of wavelet coefficients is observed at damage location for every scale. At the same time, local peaks or ridges can be observed due to noise at different locations and for certain scales. The peak values of wavelet coefficients due to noise can be higher than the peak values due to damage, but the criteria for identifying the damage location is a singular behavior for all the scales.

Thus, the normalized scalograms make it easier to observe the results for each scale of the scalogram and to eventually discern between the effect of possible damage and

Table 3: MAC values between numerical and experimental modes (undamaged state) for each mode and for each position of the roving mass.

Mass Position\Mode	1	2	3	4	5
1	0.9955	0.9988	0.9973	0.9950	0.9919
2	0.9957	0.9983	0.9976	0.9956	0.9694
3	0.9963	0.9985	0.9970	0.9950	0.9925
4	0.9964	0.9989	0.9977	0.9959	0.9833
5	0.9951	0.9988	0.9976	0.9957	0.9877
6	0.9940	0.9983	0.9973	0.9946	0.9908
7	0.9906	0.9989	0.9977	0.9956	0.9852
8	0.9979	0.9990	0.9977	0.9954	0.9913
9	0.9909	0.9987	0.9980	0.9944	0.9875
10	0.9967	0.9987	0.9981	0.9955	0.9872
11	0.9981	0.9983	0.9970	0.9930	0.9855

Table 4: SNR values [dB] of experimental modes with respect to numerical modes (undamaged state) for each position of the roving mass.

Mass Position\Mode	1	2	3	4	5
1	55	67	59	52	48
2	51	63	60	54	40
3	54	65	58	53	48
4	55	68	60	54	40
5	53	66	60	54	43
6	58	63	59	52	46
7	46	68	60	54	42
8	63	69	60	53	47
9	46	66	62	51	43
10	53	66	62	54	43
11	55	63	58	50	42

noise. However, as a consequence, the normalization process can make the scalogram to look similar for different scales. The information of the values of the wavelet coefficients at every scale is lost because of the normalization, but the damage identification process analyzes the relative peaks of wavelet coefficients at every scale, instead of their actual values.

In the normalized scalograms, if no noise was present, clear peaks would be observed solely at damage locations for all scales. In real applications, when noise is present, additional peak values can be observed at different locations and at certain scales. From a practical point of view, the challenge is to make the effect of noise as small as possible, in order to avoid masking the actual effect of damage. If the noise level is high (or the

Table 5: SNR values [dB] of experimental modes (undamaged state) with respect to their corresponding cubic spline approach for each position of the roving mass.

Mass Position\Mode	1	2	3	4	5
1	57	69	67	62	59
2	57	58	68	60	58
3	53	61	62	57	57
4	54	68	68	59	58
5	54	62	68	60	58
6	57	66	65	58	59
7	60	61	66	60	57
8	56	68	64	60	58
9	54	63	64	60	59
10	58	69	68	57	54
11	57	70	64	54	57

damage severity is small), the high values of wavelet coefficients may extend in the scale dimension and lead to 'false positives' (possible damages identified at locations where is no damage). This phenomenon may also occur when the source of the noise is not random but it is due to a specific reason at a certain location (for instance a faulty sensor, cable, etc.)

The presented damage detection approach is aimed at reducing the effect of noise so more clear scalograms are obtained for damage detection, in order to enhance the sensitivity to damage. The performance and limits of the proposed methodology are explored in this section. Results are presented for all identified modes and for all scales for different damage scenarios, in order to illustrate the capabilities of the method in a real application where no prior information is known about the properties of any existing damage.

It can be seen from Figure 7 that when the crack is very small (only 10% of the height of the beam), the damage can not be detected except from mode 2. As it was shown in the previous section (Table 4), this mode is indeed the least contaminated by noise, so it indicates that noise is probably masking the effect of damage in the rest of mode shapes. The level of noise is also relevant enough to contaminate the results obtained from the combination of all modes. In addition, mode 2 indicates the true damage location at 0.4L which is in a region where this mode exhibits maximum amplitude and therefore it is sensitive to damage. Thus, taking into account both features (low noise and damage in a sensitive area), it can be concluded that mode 2 is providing a reliable damage detection result.

Figure 8 shows that when damage is more severe the damage is also detected by mode 3 (Figure 8.(c)) and less clearly by mode 5 (Figure 8.(e)). However, mode 2 gives the most reliable information because of its sensitivity and its low noise. Thus, the result obtained when combining all modes (Figure 8.(f)) is very similar to the one obtained with mode 2.

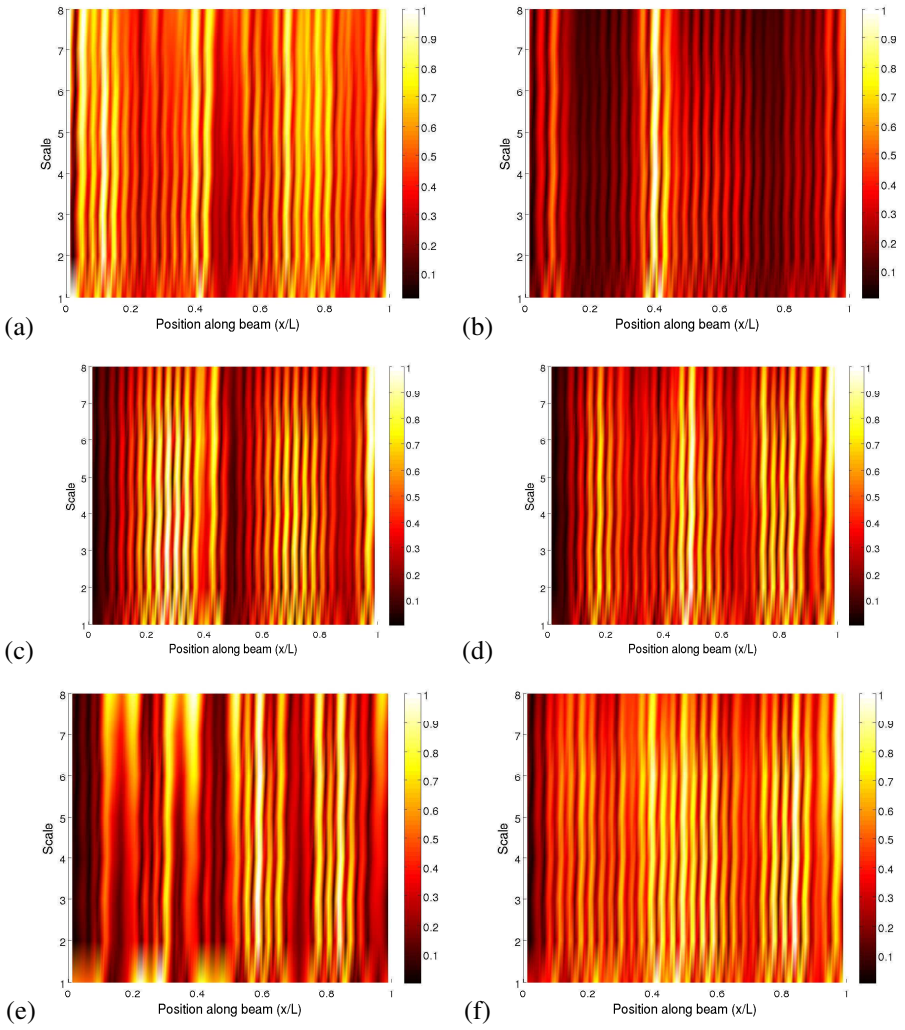

Figure 7: Normalized weighted addition of wavelet coefficients for crack depth 10% and 5% mass for (a) mode 1, (b) mode 2, (c) mode 3, (d) mode 4, (e) mode 5 and (f) combination of all mode shapes.

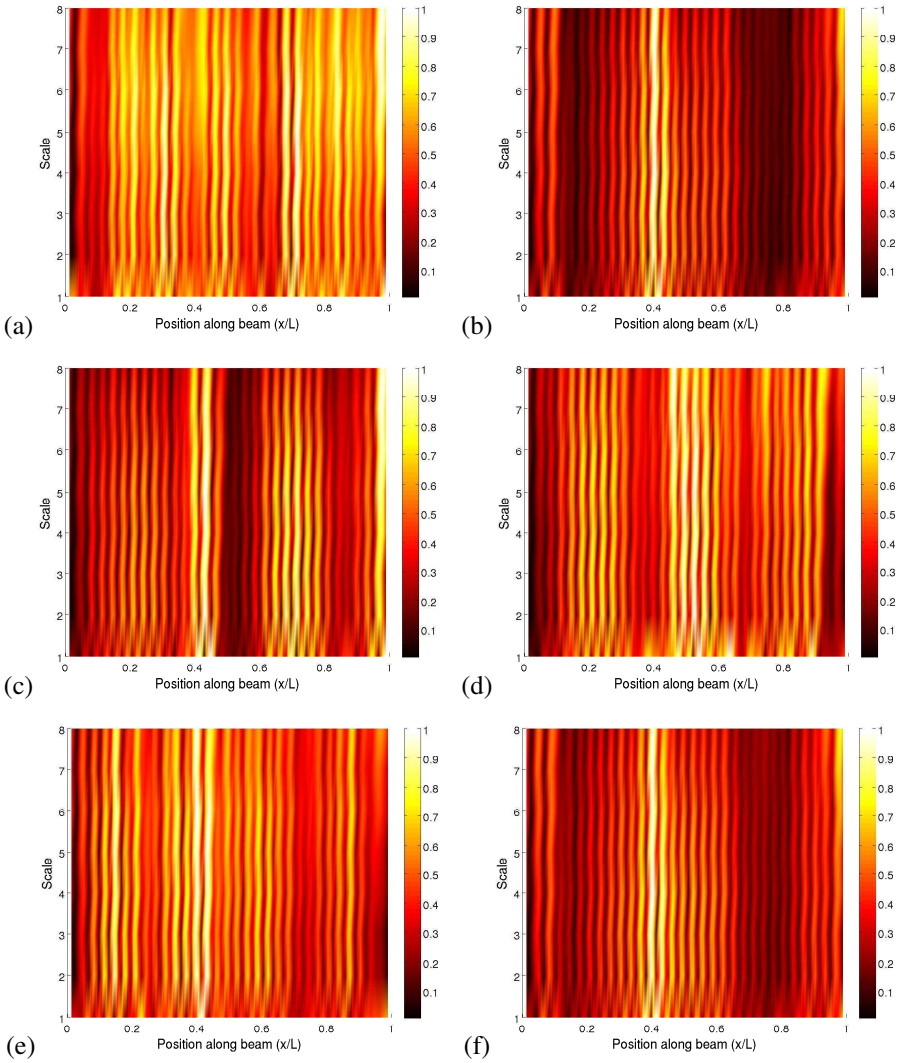

Figure 8: Normalized weighted addition of wavelet coefficients for crack depth 20% and 5% mass for (a) mode 1, (b) mode 2, (c) mode 3, (d) mode 4, (e) mode 5 and (f) combination of all mode shapes.

For the most severe damage scenario, modes 2 and 5 (Figure 9.(b) and Figure 9.(e)) are again sensitive to damage, whereas mode 3 (Figure 9.(c)) can not detect damage.

Mode 4 (Figures 7.(d), 8.(d) and 9.(d)) is not pointing to the damage location even though it also exhibits high modal amplitudes at damage location. This is likely to be due to noise in the mode shape, so the effect of noise is masking the effect of damage. However, this noise effect is diminished when results from all mode shapes are combined because of the weighting coefficient based on the SNR of each mode shape.

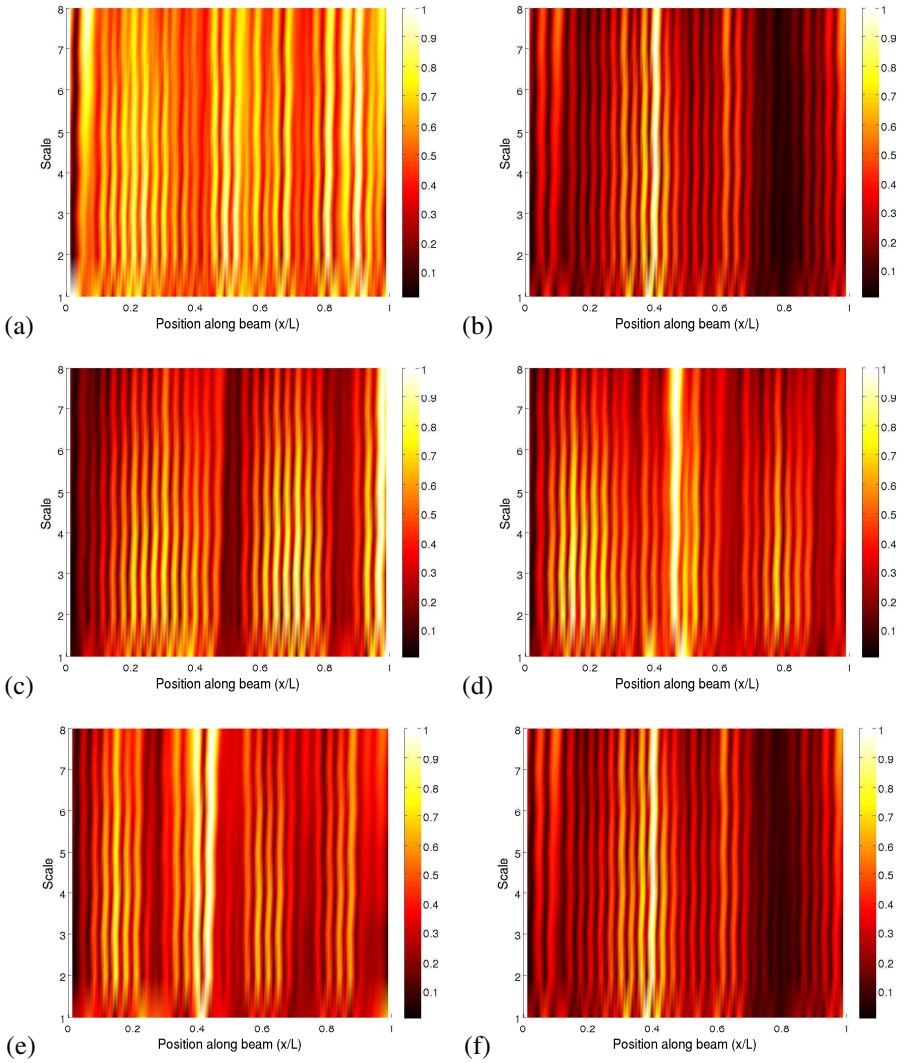

Figure 9: Normalized weighted addition of wavelet coefficients for crack depth 50% and 5% mass for (a) mode 1, (b) mode 2, (c) mode 3, (d) mode 4, (e) mode 5 and (f) combination of all mode shapes.

Figure 10 shows the results for a crack depth of 50% when using a higher value of the roving mass (10% of the mass of the beam). It can be seen that the results are very similar to those obtained for the 5% mass (Figure 9). Theoretically, a higher value of the mass increases the effect of the attached mass on the structural response and therefore can highlight more clearly the effect of damage. On the other hand, if the mass is too small, it may not make any difference on the structural response and it turns out to be useless. However, from a practical point of view, the value of the mass is limited because its

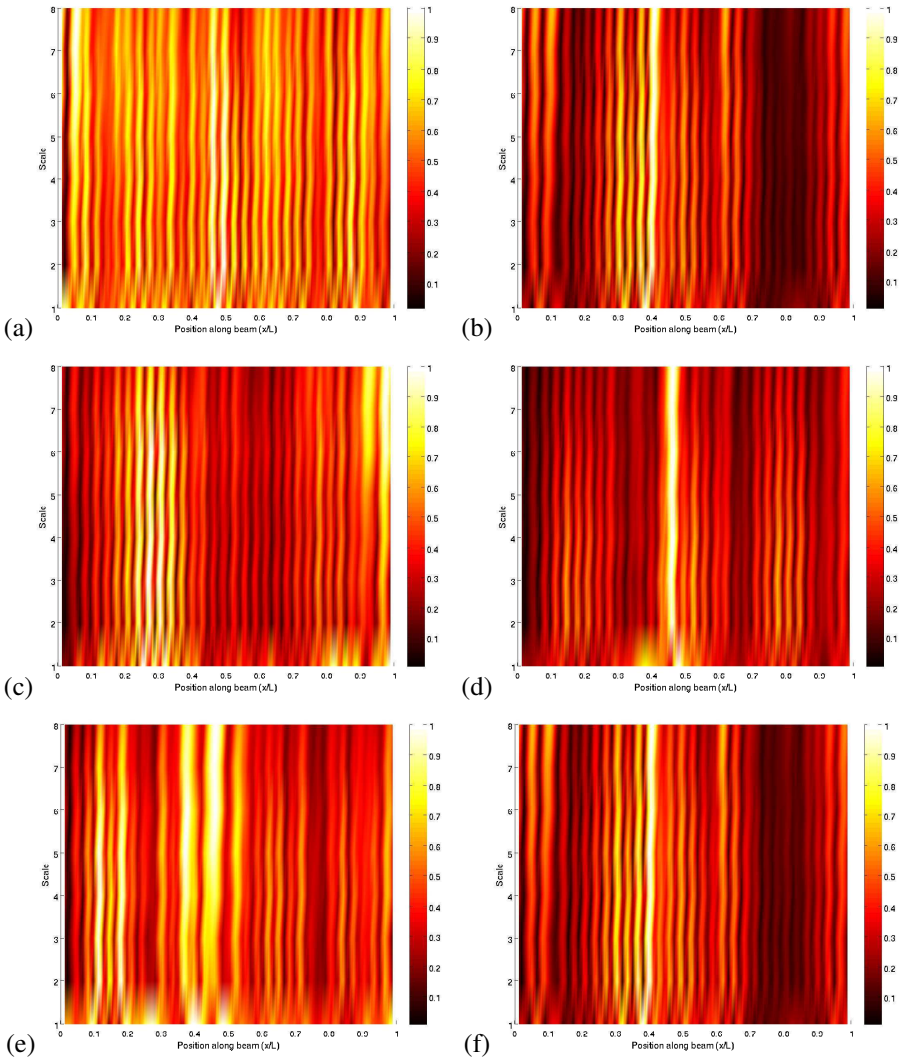

Figure 10: Normalized weighted addition of wavelet coefficients for crack depth 50% and 10% mass for (a) mode 1, (b) mode 2, (c) mode 3, (d) mode 4, (e) mode 5 and (f) combination of all mode shapes.

size may be too big, and it may be difficult to handle and to be attached to the structure. These factors may even lead to some undesirable consequences such as inducing non-linear effects because of contact or geometrical non-linearities. Therefore, there is a trade off between the practical size of mass and its effect on the structure. According to the presented results, values between 5 and 10% provide successful results.

Figure 11 shows the results obtained for a crack of 50% depth when no roving mass is used. By comparing Figures 9, 10 and 11 it can be seen that the use of the roving

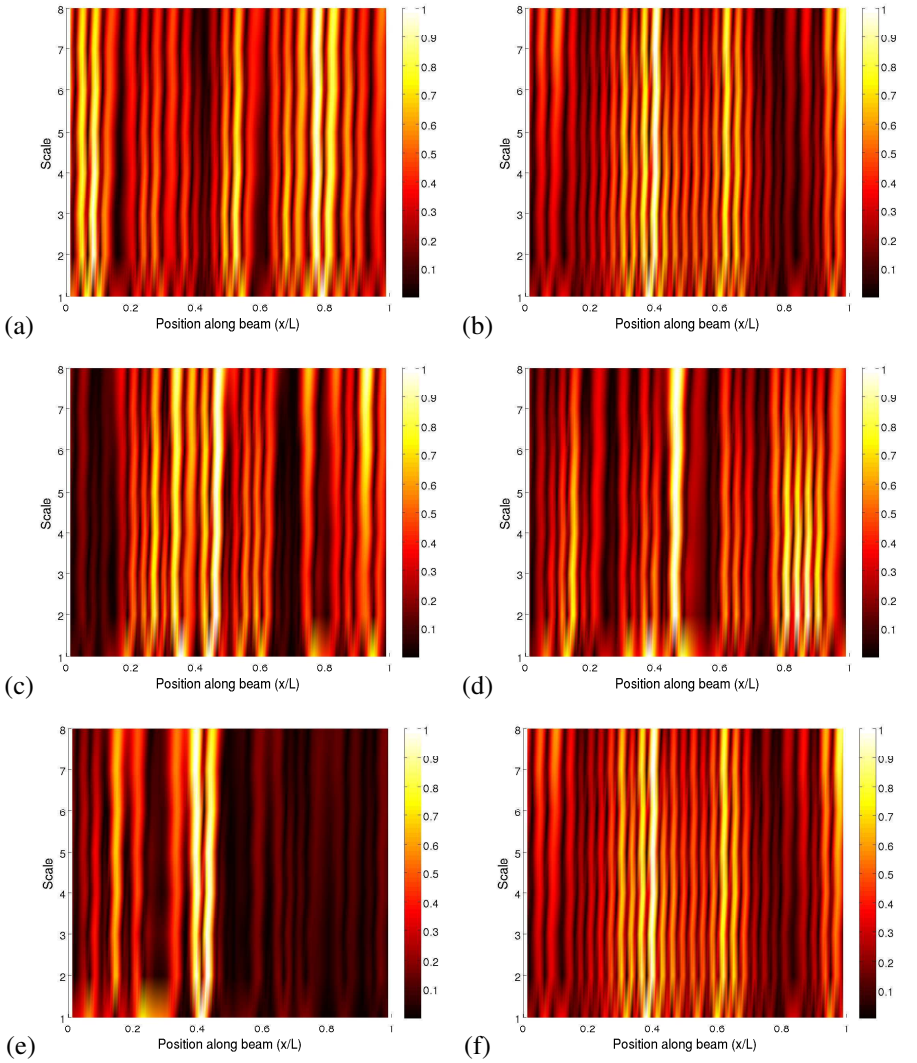

Figure 11: Normalized weighted addition of wavelet coefficients for crack depth 50% and no roving mass for (a) mode 1, (b) mode 2, (c) mode 3, (d) mode 4, (e) mode 5 and (f) combination of all mode shapes .

mass reduces the effect of noise and increases the sensitivity to damage for mode 2, the one with lowest noise level. Moreover, the result of the combination of all modes with the roving mass is clearer than the one without roving mass. Hence, the use of the roving mass is useful for mitigating the effect of noise.

In order to illustrate the effect of the wavelet choice in the final results, Figure 12 shows the result of the combination of all mode shapes for all mass positions for a 50% crack and 5% mass when different wavelets are considered: Gauss with 2 vanishing

moments, Coiflet with 2 and 4 vanishing moments and Daubechies with 3 and 4 vanishing moments. The presented results show that similar results are obtained for all the considered wavelet function with 2 vanishing moments. However, slightly better results are obtained for the Daubechies (Figure 9(f)) than for Gauss (Figure 12(a)) and Coiflet (Figure 12(b)). When the number of vanishing moments increases, the oscillatory nature of the wavelet function expands and the effect of the damage in the scalogram is also slightly expanded (Figure 12(c), (d) and (e)). These results are consistent with those presented in [16].

In order to show the performance of the method with smaller number of measuring points, Figure 13 shows the results when only one set-up of sensors (16 measuring points) is used. The results show that the method is able to detect damage when using even such a small number of sensors. For the 10% crack, the results are even better than when 32 sensors are used (Figure 7(a)). Even though the sensitivity to damage detection is theoretically improved by increasing the number of sensors, however, if less sensors are used, it is possible that there are less noisy data and whereas the effect of damage is still detected by the remaining sensors. This phenomenon has been previously reported in [16].

Conclusions

This paper applies a damage detection technique based on the wavelet analysis of the mode shapes obtained from healthy and damaged states. The experimental results indicate that the method can successfully detect the damage location (even when it is in the middle of two adjacent measuring points). The results also show how the noise for each mode influences the performance of this damage identification methodology. The least noisy modes are the most reliable ones, especially in the areas where they show maximum amplitudes.

For the experimental tests included in the paper, results from mode 2 for all three damage scenarios clearly offer the correct damage location, while the modes with higher noise level did not provide much useful information since the damage effect was masked by the noise. Therefore the estimated level of noise (SNR) should be used for a rigorous analysis. Except for the 10% severity damage, the combination of wavelet coefficients of all modes provides a more reliable result for the damage detection than each mode individually. Nevertheless, both the combined results and the results from modes with lower noise level should be investigated in the analysis since the combined result may not be sensitive to light level of structural damage. In addition, when the roving mass is used, the summation process reduces the effect of noise and increase the sensitivity of the methodology to damage.

Thus, the main original contributions of the paper (namely the use of estimated SNR in mode shapes and the roving mass) can be applied to other damage detection approaches in 1D, 2D or 3D structures to enhance their sensitivity to damage. The obtained results can also be better than those presented in this paper if more measuring points are used, higher order modes are identified, the accuracy of the measuring system is better, etc. The effect of prestressing in the proposed methodology should be studied from the experimental analysis of concrete beams.

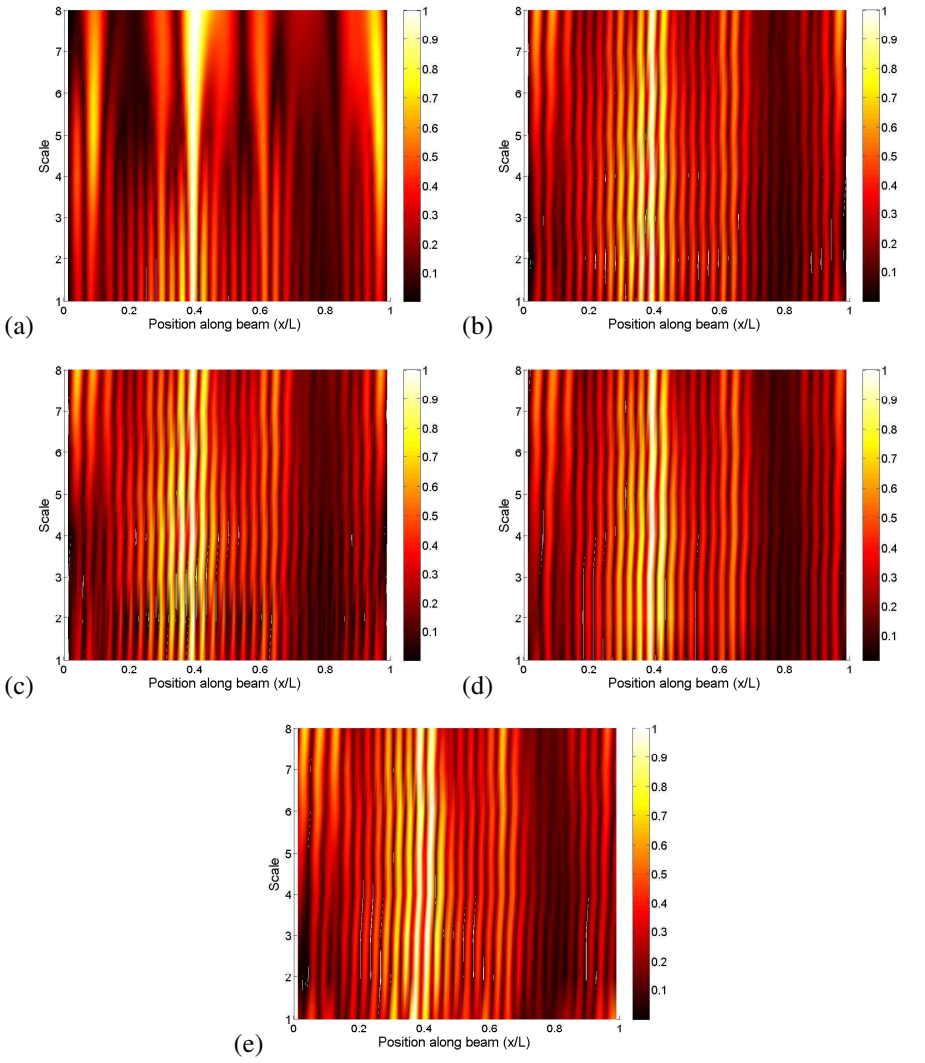

Figure 12: Normalized weighted addition of wavelet coefficients for all mode shapes for crack depth 50% and 5% mass using wavelet (a) Gauss with 2 vanishing moments, (b) Coiflet with 2 vanishing moments, (c) Coiflet with 4 vanishing moments, (d) Daubechies with 3 and (e) Daubechies with 4 vanishing moments.

Acknowledgments

The authors deeply appreciate all the reviewers' and editor comments, ideas and suggestions, which have certainly permitted to raise the manuscript quality.

This work was supported by the Consejería de Economía, Innovación, Ciencia y Empleo of Andalucía (Spain) under project P12-TEP-2546 and the Ministerio de Eco-

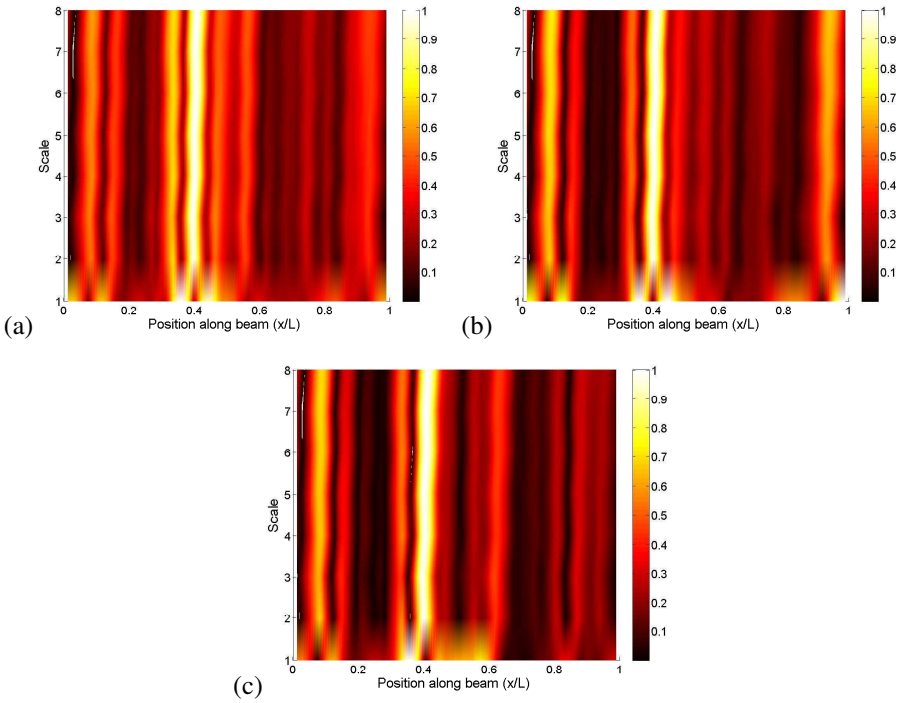

Figure 13: Normalized weighted addition of wavelet coefficients for all mode shapes for 5% added mass using wavelet Daubechies with 2 vanishing moments and 16 sensors for (a) 10% crack, (b) 20% crack and (c) 50% crack.

nomía y Competitividad through research projects BIA2013-43085-P and BIA2016-75042-C2-1-R. Financial support is gratefully acknowledged.

References

1. Fan, W. and Qiao, P. Vibration-based Damage Identification Methods: A Review and Comparative Study. Struct. Health Monit., 10(1):83–111, 2011.
2. A. Panopoulou, S. Fransen, V. Gomez-Molinero, and V. Kostopoulos. Experimental modal analysis and dynamic strain fiber Bragg gratings for structural health monitoring of composite antenna sub-reflector. CEAS Space J., 5(1-2):57–73, 2013.
3. I. García, J. Zubia, G. Durana, G. Aldabaldetreku, M.A. Illarramendi, and J. Villatoro. Optical Fiber Sensors for Aircraft Structural Health Monitoring. Sensors, 15(7):15494–15519, 2015.
4. G Strang and T Nguyen. Wavelets and Filter Banks. Wellesley- Cambridge Press, 1996.
5. C Surace and R Ruotolo. Crack detection of a beam using the wavelet transform. In Proceedings of the 12th International Modal Analysis Conference, pages 1141–1147, 1994.
6. M. M. R. Taha, A. Noureldin, J. L. Lucero, and T. J. Baca. Wavelet Transform for Structural Health Monitoring: A Compendium of Uses and Features. Struct. Health Monit., 5(3):267–295, 2006.
7. A. Katunin. Modal-Based Non-Destructive Damage Assessment in Composite Structures Using Wavelet Analysis: A Review. Int. J. Compos. Mat., 3(6B):1–9, 2013.

8. M. Rucka. Damage detection in beams using wavelet transform on higher vibration modes. J. Theor. Appl. Mech., 49(2):399–417, 2011.
9. M. Cao, M. Radzieński, W. Xu, and W. Ostachowicz. Identification of multiple damage in beams based on robust curvature mode shapes. Mech. Syst. Signal Proc., 46(2):468–480, 2014.
10. M.D. Ulriksen and L. Damkilde. Structural damage localization by outlier analysis of signal-processed mode shapes âŁ“ Analytical and experimental validation. Mech. Syst. Signal Proc., (68-69):1–14, 2016.
11. P. Rajendran and S. M. Srinivasan. Identification of added mass in the composite plate structure based on wavelet packet transform. Strain, 52(1):14–25, 2016. STRAIN-1064.R1.
12. A. Katunin and P. Przystalka. Damage assessment in composite plates using fractional wavelet transform of modal shapes with optimized selection of spatial wavelets. Eng. Appl. Artif. Intell., 30:73–85, 2014.
13. A. Katunin, M. Dańczak, and P. Kostka. Automated identification and classification of internal defects in composite structures using computed tomography and 3D wavelet analysis. Arch. Civ. Mech. Eng., 15(2):436–448, 2015.
14. A. Katunin. Stone impact damage identification in composite plates using modal data and quincunx wavelet analysis. Arch. Civ. Mech. Eng., 15(1):251–261, 2015.
15. L. Montanari, A. Spagnoli, B. Basu, and B. Broderick. On the effect of spatial sampling in damage detection of cracked beams by continuous wavelet transform. J. Sound Vibr., 345:233–249, 2015.
16. M. Solís, M. Algaba, and P. Galvín. Continuous wavelet analysis of mode shapes differences for damage detection. Mech. Syst. Signal Proc., 40(2):645–666, 2013.
17. S. Zhong and S. O. Oyadiji. Analytical predictions of natural frequencies of cracked simply supported beams with a stationary roving mass. J. Sound Vibr., 311(1-2):328–352, 2008.
18. S. Zhong, S. O. Oyadiji, and K. Ding. Response-only method for damage detection of beam-like structures using high accuracy frequencies with auxiliary mass spatial probing. J. Sound Vibr., 311(3-5):1075–1099, 2008.
19. A. V. Ovanesova and L. E. Suárez. Applications of wavelet transforms to damage detection in frame structures. Eng. Struct., 26(1):39–49, 2004.
20. W.-X. Ren and Z.-S. Sun. Structural damage identification by using wavelet entropy. Eng. Struct., 30(10):2840–2849, 2008.
21. Y.F. Xu, W.D. Zhu, J. Liu, and Y.M. Shao. Identification of embedded horizontal cracks in beams using measured mode shapes. J. Sound Vibr., 333(23):6273–6294, 2014.
22. M. Rucka and K. Wilde. Application of continuous wavelet transform in vibration based damage detection method for beams and plates. J. Sound Vibr., 297(3-5):536–550, 2006.
23. S. Mallat. A Wavelet Tour of Signal Processing. Academic Press, London, 1999.
24. A. Gentile and A. Messina. On the continuous wavelet transforms applied to discrete vibrational data for detecting open cracks in damaged beams. Int. J. Solids Struct., 40(2):295–315, 2003.
25. X. Shao and C. Ma. A general approach to derivative calculation using wavelet transform. Chemometrics and Intelligent Laboratory Systems, 69(1-2):157–165, 2003.
26. S. Zhong and S. O. Oyadiji. Detection of cracks in simply-supported beams by continuous wavelet transform of reconstructed modal data. Comput. Struct., 89(1-2):127–148, 2011.
27. J.F. Unger, A. Teughels, and G. De Roeck. System Identification and Damage Detection of a Prestressed Concrete Beam. Journal of Structural Engineering, 132(11):1691–1698, 2006.
28. M.P. Limongelli, D. Siegert, E. Merliot, J. Waeytens, F. Bourquin, R. Vidal, V.L. Corvec, I. Gueguen, and L.M. Cottineau. Damage detection in a post tensioned concrete beam - Experimental investigation. Engineering Structures, 128(Supplement C):15–25, 2016.
29. M. Solís, A. J. Benjumea, M. Algaba, and P. Galvín. Analysis of stationary roving mass effect for damage detection in beams using wavelet analysis of mode shapes. Journal of Physics: Conference Series, 628:012014, 2015.
30. J. S. Bendat and A. G. Piersol. Random Data: Analysis and Measurement Procedures. Wiley Series in Probability and Statistics. Wiley, 2011.
31. Yonghua Jiang, Baoping Tang, Yi Qin, and Wenyi Liu. Feature extraction method of wind turbine based on adaptive Morlet wavelet and SVD. Renewable Energy, 36(8):2146–2153, 2011.
32. Ting-Hua Yi, Hong-Nan Li, and Xiao-Yan Zhao. Noise smoothing for structural vibration test signals using an improved wavelet thresholding technique. Sensors (Basel, Switzerland), 12(8):11205–20, 2012.
33. P. Guillaume, P. Verboven, S. Vanlanduit, H. Van Der Auweraer, and B. Peeters. A poly-reference implementation of the least-squares complex frequency-domain estimator. In Proceedings of 21st International Modal Analysis Conference, volume 21, pages 183–192, 2003.
34. B. Yang. Stress, Strain, and Structural Dynamics. Elsevier, 2005.

35. W. Xu, M. Cao, W. Ostachowicz, M. Radzieński, and N. Xia. Two-dimensional curvature mode shape method based on wavelets and Teager energy for damage detection in plates. Journal of Sound and Vibration, 347:266–278, 2015.
36. U. Andreaus, P. Baragatti, P. Casini, and D. Iacoviello. Experimental damage evaluation of open and fatigue cracks of multi cracked beams by using wavelet transform of static response via image analysis. Structural Control and Health Monitoring, 24(4), 2017.